

Quantitative study of the influence of swimming therapy on osteoporosis rat models based on synchrotron radiation computed tomography

Liya Huang,^a Jun Xu,^b Han Guo,^c Yujie Wang,^d Jun Zhao^a and Jianqi Sun^{a*}

Received 4 September 2017

Accepted 16 February 2018

Edited by P. A. Pianetta, SLAC National Accelerator Laboratory, USA

Keywords: swimming; different intensities; bone strength.

^aSchool of Biomedical Engineering and Med-X Research Institute, Shanghai Jiao Tong University, 800 Dongchuan Road, Shanghai, People's Republic of China, ^bDepartment of Orthopaedics, Shanghai No. 6 People's Hospital, 600 Yishan Road, Shanghai, People's Republic of China, ^cShanghai Synchrotron Radiation Facility, Shanghai Institute of Applied Physics, Cas, 239 Zhangzheng Road, Shanghai, People's Republic of China, and ^dSchool of Physics and Astronomy, Shanghai Jiao Tong University, 800 Dongchuan Road, Shanghai, People's Republic of China.

*Correspondence e-mail: milesun@sjtu.edu.cn

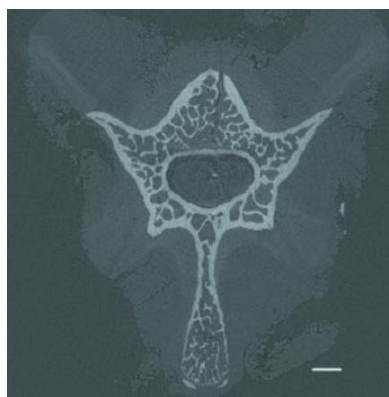
Osteoporosis is a bone disease with a variety of causes, leading to bone pain and fragility to fracture. Major treatment methods include nutrition therapy, exercise therapy, drug therapy and surgical treatment, among which exercise therapy, such as swimming, is the most effective. To investigate the optimal swimming therapy regime for postmenopausal women, the effects of eight weeks of different intensity swimming exercises were studied in rat models. After the swimming program, lumbar vertebrae were dissected from all the rats and scanned by synchrotron radiation computed tomography (SRCT). Histomorphometry analysis and finite-element analysis were carried out on the trabecular structure of the L4 lumbar based on the acquired SRCT slices. Histomorphometry analysis showed that swimming can alleviate the decrease in bone strength induced by estrogen deficiency, and moderate-intensity swimming was found to have the most significant effect.

1. Introduction

Osteoporosis is a chronic disease which leads to an increased risk of bone fracture. It is characterized by low bone mass and weakened mechanical bone strength. Resulting from estrogen deficiency at the menopause, which accelerates the loss of bone, postmenopausal women are at a higher risk of incidence of osteoporosis compared with men. Among the elderly over 50 years old worldwide, approximately one-third of women and one-fifth of men have suffered from osteoporotic fractures (Melton *et al.*, 1992, 1998; Kanis *et al.*, 2000). Therefore, the prevention and medical treatment of osteoporosis are becoming of increasing concern to the general public.

Conventionally, physical exercise is utilized as a means of intervention and treatment of osteoporosis. In past studies, commonly adopted exercises have included walking, running and some other forms of weight-bearing exercise (Omi, 2014; Kano, 1998; Wallace & Cumming, 2000; Wolff *et al.*, 1999; Block *et al.*, 1989). However, bone injuries often occur during these exercises. Swimming, on the other hand, provides sufficient physical exercise for many elderly people and is immune from the risk of injury. Therefore, swimming is increasingly recommended as an alternative exercise therapy for many elderly people.

Previously, swimming, as a non-weight-bearing exercise, was considered as possibly having an unfavorable effect on bone, and thus very few studies were conducted in either humans or animals in the past to explore the impact of



swimming on bone health. Swissa-Sivan *et al.* reported that swimming positively affected the growth and development of bone in young rats significantly, but the effects on young adult rats were not significant (Swissa-Sivan *et al.*, 1989, 1990). Hoshi *et al.* revealed a significant increase in femoral bone density but few changes in the mechanical properties of bone in swim-trained mice, and the effects of swimming in female mice were greater than those in males (Hoshi *et al.*, 1996, 1998). Snyder *et al.* performed swimming and running exercises of equal duration and intensity on female rats, and the results demonstrated that swimming is more effective for bone development (Snyder *et al.*, 1992). Nyska *et al.* showed that swimming yielded greater histomorphometric changes in young adult rats (Nyska *et al.*, 1995).

However, little information exists about the effects of swimming exercise on bone health after menopause. Osteoporosis in ovariectomized rats has been widely used as a model for postmenopausal osteoporosis in the human, as estrogen deficiency induced by ovariectomy resembles the postmenopausal state (Kalu, 1991; Miller *et al.*, 1995). On the other hand, one important issue which has been normally overlooked in the study of the effect of swimming on bone health is the optimal training intensity. Bone adaptation in response to stress and strain evoked by exercise seems to be different at different swimming intensities (Swissa-Sivan *et al.*, 1989; Armstrong *et al.*, 1974).

The purpose of this study is to investigate the effects of different intensities of swimming exercises on bone health, and seek for the optimal training regime to increase bone mass and enhance mechanical bone strength, thus providing evidence for early prevention and medical treatment of postmenopausal osteoporosis by swimming exercise.

2. Materials and methods

2.1. Experimental animals

Twenty-four three-month-old female Sprague-Dawley rats, of mean weight 200 ± 15 g, were used in this study. The study was approved by the Institutional Animal Care of Shanghai Jiao Tong University. All the rats were raised under standard laboratory conditions in the Laboratory Animal Center of Shanghai Jiao Tong University. Temperature was maintained at $\sim 22\text{--}23^\circ\text{C}$, and the rats were subjected to a 12 h light/dark cycle. During the experiment, all the rats were provided with a standard solid diet and water *ad libitum*.

After an acclimatization period of two weeks, the rats underwent experimental procedures. They were randomly assigned to two groups: an ovariectomized (OVX) group with 20 rats and a sham operated (sham) group with four rats. For the OVX group, the rats were firstly anesthetized and then underwent ovariectomy bilaterally with a ventral approach. For the sham group, two small blocks of fat near the ovary,

Table 1
Scheme of adaptive training.

Group	Percent of dead weight loaded during swimming (%), duration of training (min)						
	Day 1	Day 2	Day 3	Day 4	Day 5	Day 6	Day 7
LFE	0, 20	0, 30	0, 40	0, 45	0, 50	0, 55	0, 60
LIE	0, 20	0, 30	0, 40	3%, 30	3%, 40	3%, 50	3%, 60
MIE	0, 20	0, 30	0, 40	3%, 30	4%, 40	5%, 50	6%, 60
HIE	0, 20	0, 30	0, 40	3%, 30	5%, 40	7%, 50	9%, 60

whose size was the same as the ovary, were removed bilaterally.

2.2. Training program

After a recovery period of one week, the OVX group were further randomly divided into five subgroups: non-exercise (control) group, load-free exercise (LFE) group, low-intensity exercise (LIE) group, moderate-intensity exercise (MIE) group and high-intensity exercise (HIE) group, and each subgroup included four rats. When swimming, the rats in groups LIE, MIE and HIE were loaded with 3%, 6% and 9% dead weight of lead at the root of their tails, respectively (Donald, 1965). Before the training program, all the exercise groups underwent adaptive training for one week. A scheme of the adaptive training is presented in Table 1, in which parameters of the percent of dead weight loaded on the rats during swimming and duration of training are listed.

The training program comprised exercising three days, resting one day, exercising two days and resting one day, which amounts to exercising five days per week for eight consecutive weeks. Exercised rats were tamed to swim continuously for 60 min on an exercising day. Swimming exercise occurred in a 1.5 m-diameter water maze, filled with 45 cm-deep lukewarm water. Water temperature was maintained at $\sim 30\text{--}35^\circ\text{C}$ for best swimming performance of the rats (Dawson & Horvath, 1970). During the exercise, the exercised rats were supervised not to touch the bottom of the water maze or hang on to other rats, and prevented from drowning. The control group were immersed in shallow water up to their neck for 60 min simultaneously with the exercised rats. The temperature of the shallow water was maintained at $\sim 30\text{--}35^\circ\text{C}$ in order to exclude the effect of temperature and water contact (Bourrin *et al.*, 1992). The sham group were kept sedentary in cages during the whole training program. All the rats were weighed once a week on the resting day, and the corresponding load weights they carried were updated with their new weight data.

At the end of the training program, 24 h after the last exercise of the exercised rats, all rats were euthanized by overdose of anesthetic. The lumbar vertebrae were dissected from all the rats and cleaned of muscle tissue and connective tissue. All excised bones were placed in 10% phosphate-buffered formalin for preservation.

2.3. Imaging

Synchrotron radiation computed tomography (SRCT) scanning of all specimens was performed at the BL13W1 beamline at Shanghai Synchrotron Radiation Facility. Three

days before scanning, all specimens were dehydrated and immobilized in centrifuge tubes of suitable size. We chose to work with a beam energy of 26 keV and a Photonic Science detector with pixel size of $9\ \mu\text{m} \times 9\ \mu\text{m}$, in order to achieve the best contrast of our SRCT images taking into account the size of the specimens. Absorption imaging methods were used in the study, so the specimens were placed as close as possible to the detector to avoid phase-contrast effects. In our study, the specimens were placed as close as possible to the detector at a distance of 11 cm due to hardware constraints. Each specimen was vertically glued on the sample stage for CT scanning. Each CT scan consisted of 1200 radiographic projections with an exposure time of 15 ms for each projection.

After image acquisition, X-ray image processing and tomography reconstruction software *PITRE* (Shanghai Institute of Applied Physics, Chinese Academy of Sciences) was used to reconstruct the bone images. The reconstruction was performed using the *Gridrec* algorithm. As a result of the good contrast of SRCT images, bone structure was easily segmented from soft tissue or background by threshold segmentation. Then median filtering with a 3×3 square structuring element was applied to binarize the images of bone.

2.4. Histomorphometry analysis

Histomorphometry analysis of bone, especially of the trabecular structure, can reveal changes of bone in two-dimensional morphological characteristics (Prot *et al.*, 2015). Histomorphometrical parameters are one of the most important parameters for bone strength evaluation in clinical research. Therefore, histomorphometry analysis was carried out on the trabecular structure of the L4 lumbar vertebra in our study (Sales *et al.*, 2012).

First, median-filtered images of bone previously obtained were stacked into three-dimensional bone images. Then, a longitudinal cuboid region of interest (ROI) including approximately $400\ 180 \times 160$ pixel slices was selected from each specimen; thus the size of the selected ROIs was approximately $1.44\ \text{mm} \times 1.62\ \text{mm} \times 3.60\ \text{mm}$. All ROIs were selected from the same anatomical position, ensuring that all ROIs analyzed in our study could be compared. Quantitative analysis software *CTAn* (Bruker Scientific Technology, Belgium) was used here to calculate the histomorphometrical parameters from selected three-dimensional trabecular ROIs.

In our study, the following histomorphometrical parameters were calculated: bone volume fraction [bone volume/tissue volume (BV/TV) (%)], bone surface to bone volume ratio [bone surface/bone volume (BS/BV) (μm^{-1})], bone surface density [bone surface/tissue volume (BS/TV) (μm^{-1})], trabecular thickness [Tb.Th (μm)], trabecular number [Tb.N (μm^{-1})] and trabecular separation [Tb.sp (μm)].

2.5. Finite-element analysis

Two-dimensional morphological parameters cannot fully reflect bone strength and usually we are more concerned with the bone's resistance ability to compression, bending and

torsion. To some extent, the biomechanical properties of bone are a better indicative parameter of fracture risk. Finite-element analysis (FEA) is a powerful and non-invasive method for simulating mechanical testing of bone, which can yield stress and strain distribution in the bone induced by load.

To gain insight into the biomechanical mechanism underlying exercise-intensity-related differences in osteoporotic vertebra strength, we conducted virtual mechanical tests on the L4 vertebrae by finite-element simulation. Owing to the high resolution of SRCT, the computational complexity of FEA increased significantly. Thus, we performed FEA on previously selected ROIs to balance computational complexity and accuracy of results.

The procedure of FEA was as follows. Firstly, an entity of the bone to be analyzed was constructed using *Mimics* 15.0 (Materialize Inc., Plymouth, MI, USA). Then, the constructed entity was repaired by deleting sharp points, filling holes, removing noise and smoothing. All these operations were implemented in *Geomagic Studio 2013* (Geomagic Inc., NC, USA), which guarantees that follow-up mesh generation can be implemented successfully. A surface mesh and volume mesh of the entity were created in *Hypermesh* 13.0 (Altair Engineering Inc., MI, USA). The generated volume mesh was imported into *ABAQUS* 6.14 (Dassault Systèmes Americas Corp, Waltham, MA, USA) to simulate mechanical testing of the bone. In the material property assignment step, an elastic modulus of 0.9 GPa and Poisson ratio of 0.3 were set specifically for the trabecular bone of vertebrae (Zhang & Fan, 2015). Material properties within the selected ROI were supposed to be homogeneous and isotropic. Then, different loads and boundary conditions were applied and set in different mechanical tests. Our FEA simulated the situation in which the biomechanical properties of the L4 lumbar vertebra work in the linear elastic range, with elastic modulus and Poisson ratio set as constant. The maximal compression force applied on the models was 25 N, which is much less than the yield load of the L4 lumbar vertebra, and strain was safely in the elastic range (Ejersted *et al.*, 1995; Cory *et al.*, 2010). Finally, the Van Mises Stress distributions and force–displacement curves could be obtained, from which the compression stiffness, bending stiffness and torsional stiffness of the vertebrae could be calculated.

2.6. Statistical analysis

In our study, *SPSS* version 16.0 (*SPSS*, Chicago, IL, USA) was applied to perform the statistical analysis. All experimental data are expressed here as mean \pm standard deviation. A one-way Anova analysis was performed to determine statistical differences between groups on all measurement parameters. A difference with $p < 0.01$ was considered statistically significant for all analyses.

3. Results

SRCT reconstructed images of L4 lumbar vertebrae for the sham, control, LFE, LIE, MIE and HIE groups are shown

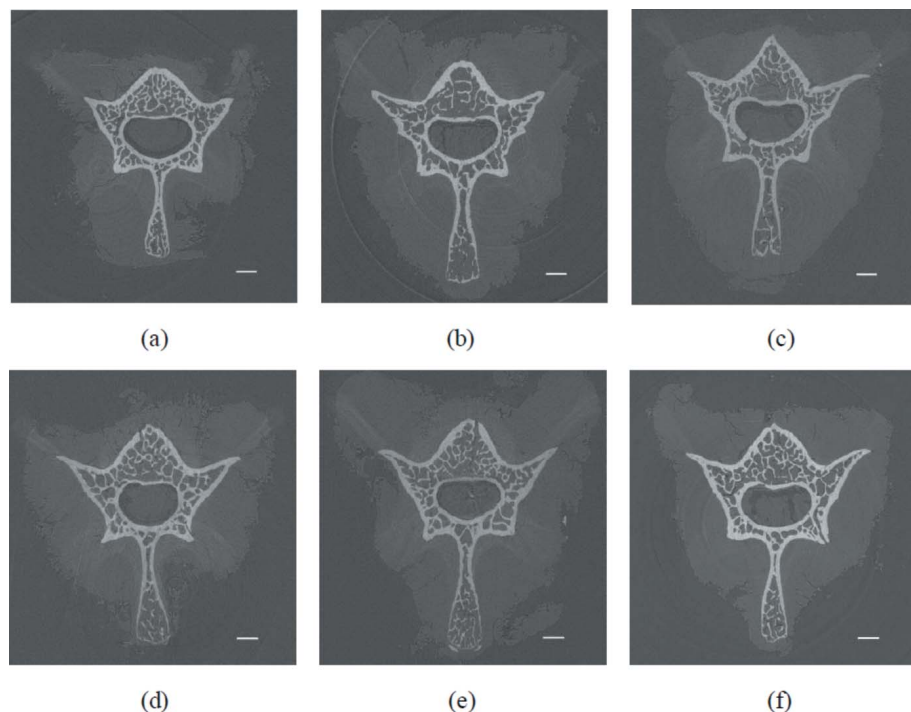


Figure 1
SRCT reconstructed images of the L4 lumbar vertebra for each group of rats: (a) sham group, (b) control group, (c) LFE group, (d) LIE group, (e) MIE group, (f) HIE group. Scale bar: 1 mm.

in Fig. 1. Obviously the interspacing of the trabecular structure in osteoporotic bone became larger due to estrogen deficiency. Nowadays, pathological examination is still the gold standard for evaluating bone structure. Therefore, we show a comparison between pathological examination and SRCT reconstructed images of the sham, control and MIE groups in Fig. 2. As can be seen, the results of the SRCT reconstructed images are nearly in accordance with the results of the pathological examination. Figs. 1 and 2 indicate that the trabecular number and trabecular thickness decreased, the trabecular separation increased and the trabecular connectivity was poorer for the control group compared with the sham group. However, the trabecular number increased, the trabecular separation decreased and the trabecular connectivity improved in the exercised groups, in general. However, it is difficult to determine the difference between exercised groups and the control group simply based on the reconstructed images. Therefore, in order to obtain more accurate results, quantitative study is indispensable.

3.1. Histomorphometry analysis

The calculated histomorphometrical parameters are summarized in Table 2 and depicted in Fig. 3. As can be seen, the bone volume fraction BV/TV, which reflects the quantity of bone, decreased greatly in all other groups compared with the sham group. The decreases in BV/TV in exercised groups were alleviated compared with the control group, with the MLE group showing the smallest decrease. Compared with the control group, BV/TV in the MIE group increased by 66%. Among the exercised groups, the differences in BV/TV

compared with the control group were statistically significant only for the MLE and HIE groups. In this experiment there exist no consistent and significant differences in BS/BV among all groups, demonstrating that swimming training does not seem to affect the BS/BV of the lumbar vertebra. As for BS/TV, all other groups were substantially lower than the sham group and the exercised groups were significantly higher or tended to be higher than the control group. Among the exercised groups, the increase for both MIE and HIE groups is statistically significant, but the value of BS/TV in the MIE group was maximal, increasing by approximately 40%. In addition, no consistent and significant changes were found in the trabecular thickness among all groups. The number of trabecular will decrease in osteoporotic bone, which can be found from comparisons of Th.N between the sham group and others. Among them, Th.N in the control group reduced to 58% of that of the sham

group. However, Tb.N in the exercised groups were bigger than that of the control, reaching the largest in the MIE group, which increased by nearly 40%. These results show that

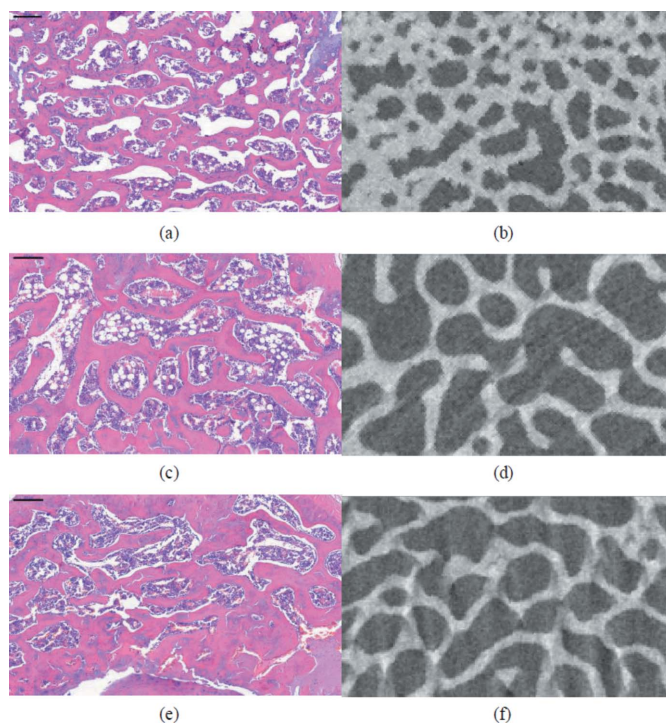


Figure 2
Comparison between pathological examination (left) and SRCT reconstructed images (right) for (a), (b) the sham group; (c), (d) the control group; (e), (f) the MIE group. Scale bar: 200 μ m.

Table 2
Morphological parameters of the L4 lumbar vertebra for each group of rats.

Group	BV/TV (%)	BS/BV (μm^{-1})	BS/TV (μm^{-1})	Tb.Th (μm)	Tb.N (μm^{-1})	Tb.sp (μm)
Sham	40.898 \pm 2.966†	0.03397 \pm 0.00381	0.01383 \pm 0.00108†	89.897 \pm 9.997	0.00457 \pm 0.00040†	183.567 \pm 14.937†
Control	20.715 \pm 1.886	0.04118 \pm 0.00154	0.00851 \pm 0.00055	78.810 \pm 1.908	0.00263 \pm 0.00018	298.702 \pm 5.403
LFE	23.984 \pm 1.917	0.04111 \pm 0.00290	0.00982 \pm 0.00041	79.637 \pm 4.6947	0.00301 \pm 0.00009	263.373 \pm 28.272
LIE	26.698 \pm 1.718	0.03623 \pm 0.00216	0.00966 \pm 0.00072	91.445 \pm 2.563	0.00292 \pm 0.00017	248.956 \pm 7.654†
MIE	34.327 \pm 2.695†	0.03454 \pm 0.00279	0.01181 \pm 0.00058†	94.426 \pm 8.893	0.00364 \pm 0.00021†	210.419 \pm 15.523†
HIE	27.659 \pm 2.67112†	0.03696 \pm 0.00467	0.01013 \pm 0.00059†	87.834 \pm 10.165	0.00316 \pm 0.00013†	251.901 \pm 10.749†

† $p < 0.01$.

swimming can alleviate the decrease of bone mass in osteoporotic bone. However, Tb.N of the vertebra only differed significantly in the MIE and HIE groups compared with the control. In osteoporotic bone, the trabecular interspacing became substantially larger, which can be illustrated from significant increases in Tb.sp in other groups compared with the sham group. Among them, Tb.sp in the control group increased by 63%. However, Tb.sp in the exercised groups was significantly lower or tended to be lower than in the control group. Tb.sp of the lumbar vertebra between the exercised and control groups were statistically significant except for the LFE group. Among the exercised groups, Tb.sp reached a minimum in the MIE group, decreasing to 70% of the control group.

3.2. Finite-element analysis

The entities of the ROIs selected in the lumbar vertebrae were meshed, and then three-dimensional finite-element models were constructed. Different mechanical tests, including compression, bending and torsion tests, were carried out on these models to simulate the vertebra's resistance ability to various external forces. Fig. 4 shows the deformation

displacements for each group under a compression force of 25 N.

The corresponding force–displacement curves or torque–angle curves, comprising information on the vertebra deformation, were recorded during mechanical tests. As shown in Fig. 5, under the same compression force the displacement in the sham group was minimal and that in the control group was maximal, while the exercised groups lie in between. Furthermore, the displacement in the MIE group was smallest among the exercised groups. These results indicate that the resistance ability of osteoporotic vertebra to compression became weaker. However, swimming could strengthen this ability, and the best effects are achieved by moderate intensity swimming exercise. In addition, the same trend occurred in bending and torsion tests. The sham group was the most difficult to bend and twist, while the control group was the easiest. Swimming could enhance the bending strength and torsional strength of osteoporotic bone, and moderate intensity swimming obtained the most significant effect.

The stiffness constants of lumbar vertebrae can be calculated as the slope of the linear part of the corresponding force–displacement curves or torque–angle curves, which are summarized in Table 3 and depicted in Fig. 6. Compared with the sham group, compression stiffness, bending stiffness and torsional stiffness in other groups decreased greatly, which was consistent with the results of force–displacement curves and torque–angle curves. However, compression stiffness, bending stiffness and torsional stiffness in the exercised groups were significantly increased or tended to increase compared with the control, indicating that swimming could alleviate the weakening effects of osteoporosis on a vertebra's mechanical strengths. For all three mechanical stiffnesses, the increases compared with the control group are statistically significant only for the MIE group.

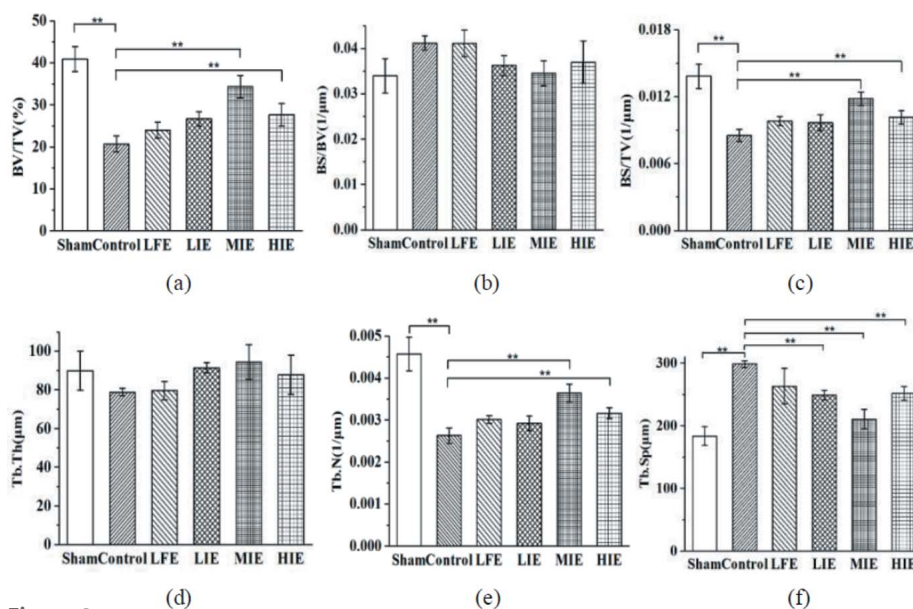


Figure 3
Comparisons of the histomorphometrical parameters of the L4 lumbar vertebra for the sham, control, LFE, LIE, MIE and HIE groups: (a) BV/TV, (b) BS/BV, (c) BS/TV, (d) Tb.Th, (e) Tb.N, (f) Tb.Sp. (** $p < 0.01$).

4. Discussion and conclusion

The results of this histomorphometry analysis and FEA of the lumbar

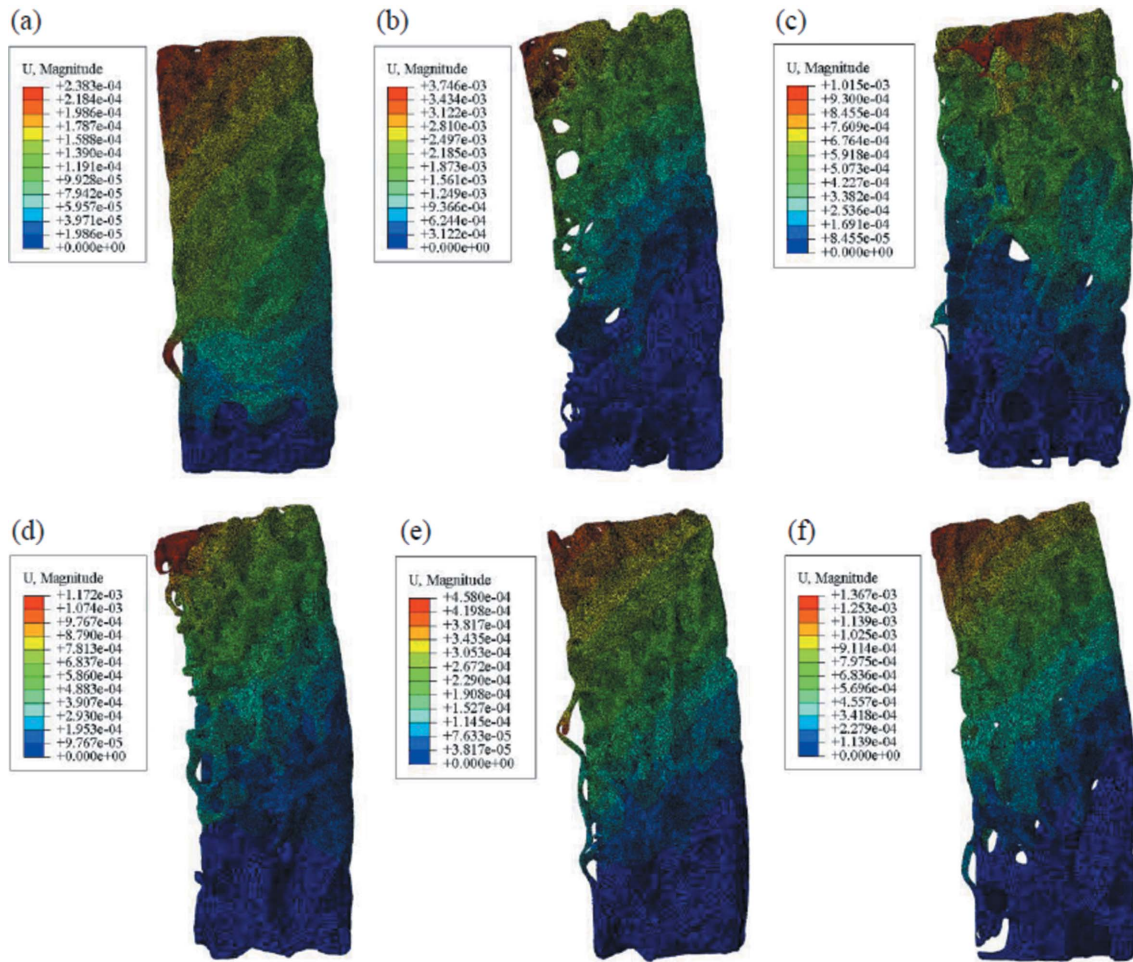


Figure 4 Deformation displacements for each group under 25 N compression force: (a) sham group, (b) control group, (c) LFE group, (d) LIE group, (e) MIE group, (f) HIE group.

vertebrae of rats suggest that swimming has a positive effect on bone mass and the mechanical properties of bone in ovariectomized rats, indicated by greater BV/TV, BS/TV, Tb.N, compression stiffness, bending stiffness and torsional stiffness and smaller Tb.sp in the exercised groups compared with in the control group. However, the extent of positive intervention effects on bone for different intensities varies. In this study the moderate intensity swimming group achieved

the most significant effect among all exercised groups. This result, that swimming exerts a positive effect on bone health, agrees with previous research results from different groups (Hart *et al.*, 2001; Omi *et al.*, 2010; Omi, 2014). In particular, it was found in this study that the weight loaded during swimming may be an important factor. Moderate intensity exercise may be the optimal choice for prevention of bone loss in ovariectomized rats treated with swimming therapy, which has

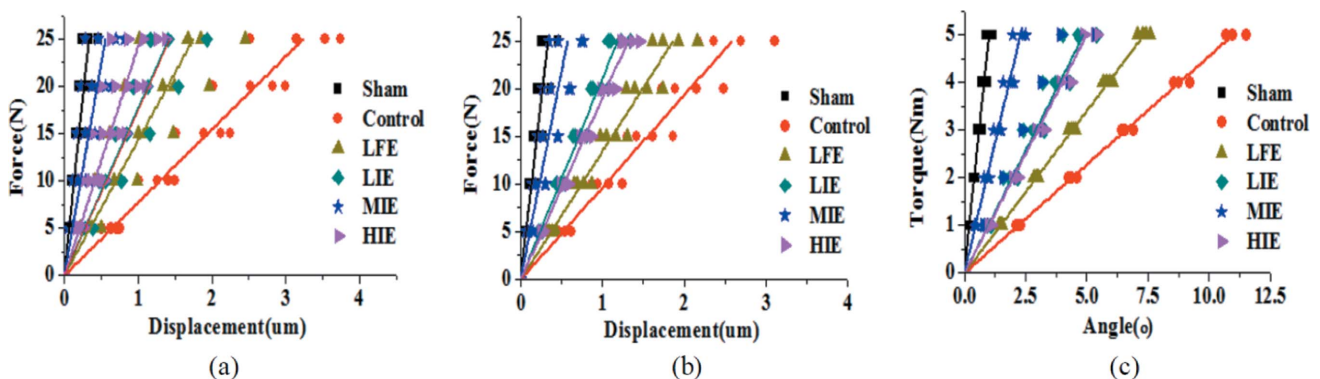


Figure 5 Force-displacement curves or torque-angle curves of the L4 lumbar vertebra for the sham, control, LFE, LIE, MIE and HIE groups. (a) Force-displacement curves in compression test. (b) Force-displacement curves in bending test. (c) Torque-angle curves in torsional test.

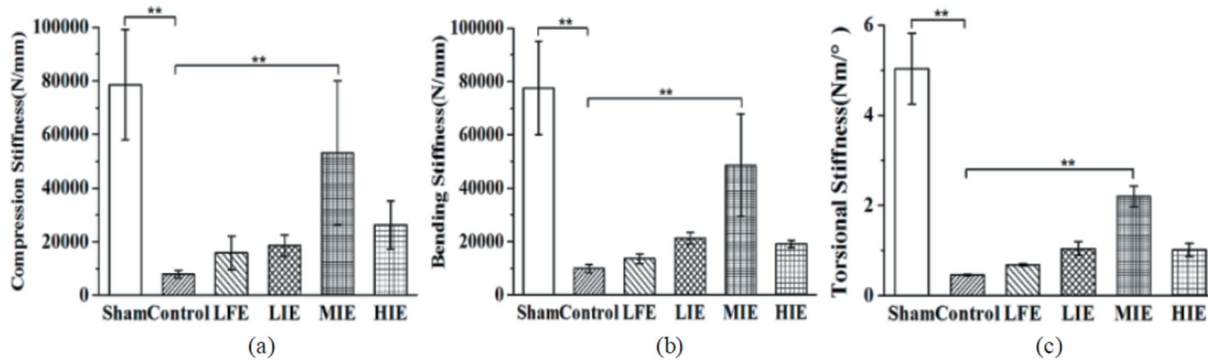


Figure 6 Comparisons of the stiffness constants of the L4 lumbar vertebra for the sham, control, LFE, LIE, MIE and HIE groups. (a) Compression stiffness. (b) Bending stiffness. (c) Torsional stiffness. (** $p < 0.01$.)

Table 3 The stiffness constants of L4 lumbar vertebra for each group of rats.

Group	Compression stiffness (N mm ⁻¹)	Bending stiffness (N mm ⁻¹)	Torsional stiffness (N m deg ⁻¹)
Sham	78487.64 ± 20571.80†	77534.44 ± 17405.59†	5.03221 ± 0.79098†
Control	7905.21 ± 1452.53	9861.07 ± 1519.87	0.45638 ± 0.01571
LFE	15821.13 ± 6210.83	13598.46 ± 1713.05	0.68253 ± 0.01972
LIE	18449.90 ± 4049.73	21262.81 ± 2157.23	1.04530 ± 0.15507
MIE	53013.27 ± 26952.82†	48594.94 ± 19195.68†	2.19672 ± 0.23075†
HIE	26224.57 ± 8887.31	19118.34 ± 1389.27	1.01665 ± 0.14473

† $p < 0.01$.

also been suggested in previous studies (Bagi *et al.*, 1992; Zhong, 2007).

A possible reason underlying the finding that moderate intensity swimming exercise is most effective for bone health is that a moderate load can provide the necessary stimulus for osteogenic effects. An ameliorating effect on bone loss is the adaptive strengthening of bone under the stress and strain evoked by exercise. During swimming with load, bone sustains more stress, strains, moments and torques due to muscle contractions. Thus bone mass and mechanical competence increase to counterbalance these exercise stimuli. The findings of this study are in accordance with the ‘Mechanostat mechanism(s)’ proposed by Frost (1990), which pointed out that bone structure will change and bone mass will increase in response to increased mechanical loading, but only if stress is beyond the ‘minimal effective signal’ value. Although increased mechanical loading can facilitate osteogenic effects, load beyond a certain threshold may depress bone modelling and promote bone remodelling, resulting in higher bone turnover. Consequently, bone mass decreases and mechanical incompetence occurs in bone. According to Harri & Kuusela (1986), the weight loaded during swimming should be less than the maximum weight with which rats can still maintain respiration during swimming. Therefore, the weight load should be in an appropriate range to achieve moderate intensity swimming exercise.

To the author’s knowledge, this study is the first to demonstrate that moderate intensity is optimal for ovariectomized rats undergoing swimming exercise, using histomorphometry analysis and FEA on the SRCT of rats’ lumbar

vertebrae. The scanning speed of conventional micro-CT is very slow, and the number of specimens needed to be scanned is very large in the current experiment. Therefore, synchrotron radiation imaging, which is a quick imaging method, is more advantageous in this study. Moreover, compared with ordinary micro-CT images, the resolution and contrast of SRCT images are higher. Therefore, details of the bone microstructure in SRCT images are more clear, and histomorphometrical parameters derived from the SRCT images are more accurate. Additionally, based on the SRCT images, more detailed structural features of bone, for example cracks or crevices, can be obtained, which could be crucial for the understanding of the mechanical strength of the bones. This information can be plugged into the FEA for a better estimation of bone strength compared with simple histomorphometrical parameters. Dual-energy X-ray absorptiometry (DXA) is clinically used to measure bone mineral density (BMD) in order to estimate bone strength. However, BMD can only account for 70% of bone strength (Löfman *et al.*, 2000). Based on information provided by DXA, virtual mechanical tests to simulate a vertebra’s resistance ability to various external forces cannot be conducted. Therefore, in this study, histomorphometry analysis is combined only with FEA.

Although this study was performed on rats, the results can be extended to humans to some extent. In conclusion, the present study demonstrates that moderate intensity swimming exercise can serve as an advisable option for the prevention and medical treatment of postmenopausal osteoporosis, which may significantly reduce fracture incidence in elderly people. In the future, investigations with both real-time mechanical tests and imaging are necessary. During image acquisition, the specimens will undergo various practical mechanical tests. Comparing actual mechanical measurements and simulation results from SRCT images could improve the accuracy of this method and establish it as a potential new standard.

Funding information

Funding for this research was provided by: National Natural Science Foundation of China (grant No. U1732119; grant No. 11575115; grant No. 813716234; grant No. U1432111); National Key Research and Development Program (grant No.

2016YFC0104608); Shanghai Jiao Tong University Medical Engineering Cross Research Funds (grant No. YG2017QN51; grant No. YG2016QN65).

References

Armstrong, R. B., Saubert IV, C. W., Sembrowich, W. L., Shepherd, R. E. & Gollnick, P. D. (1974). *Pflügers Archiv*. **352**, 243–256.
 Bagi, C. M., Miller, S. C., Bowman, B. M., Blomstrom, G. L. & France, E. P. (1992). *Bone*, **13**, 35–40.
 Block, J. E., Smith, R., Friedlander, A. & Genant, H. K. (1989). *Med. Hypotheses*, **30**, 9–19.
 Bourrin, S., Ghaemmaghami, F., Vico, L., Chappard, D., Gharib, C. & Alexandre, C. (1992). *Calcif. Tissue Int*. **51**, 137–142.
 Cory, E., Nazarian, A., Entezari, V., Vartanians, V., Müller, R. & Snyder, B. D. (2010). *J. Biomech*. **43**, 953–960.
 Dawson, C. A. & Horvath, S. M. (1970). *Med. Sci. Sports*, **2**, 51–78.
 Hardin, D. H. (1965). *Res. Q. Exercise Sport*, **36**, 370–374.
 Ejersted, C., Andreassen, T. T., Hauge, E. M., Melsen, F. & Oxlund, H. (1995). *Bone*, **17**, 507–511.
 Frost, H. M. (1990). *Anat. Rec. Adv. Integr. Anat. Evol. Biol*. **226**, 414–422.
 Harri, M. & Kuusela, P. (1986). *Acta Physiol*. **126**, 189–197.
 Hart, K. J., Shaw, J. M., Vajda, E., Hegsted, M. & Miller, S. C. (2001). *J. Appl. Physiol*. **91**, 1663–1668.
 Hoshi, A., Watanabe, H., Chiba, M. & Inaba, Y. (1996). *Environ. Health Prev. Med*. **1**, 128–132.
 Hoshi, A., Watanabe, H., Chiba, M. & Inaba, Y. (1998). *Biomed. Environ. Sci*. **11**, 243–250.
 Kalu, D. N. (1991). *Bone Miner*. **15**, 175–191.
 Kanis, J. A., Johnell, O., Oden, A., Sembo, I., Redlund-Johnell, I., Dawson, A., De Laet, C. & Jonsson, B. (2000). *Osteoporos. Int*. **11**, 669–674.

Kano, K. (1998). *J. Epidemiol*. **8**, 28–32.
 Löfman, O., Larsson, L. & Toss, G. (2000). *J. Clin. Densitom*. **3**, 177–186.
 Melton, L. J. III, Atkinson, E. J., O'Connor, M. K., O'Fallon, W. M. & Riggs, B. L. (1998). *J. Bone Miner. Res*. **13**, 1915–1923.
 Melton, L. J. III, Chrischilles, E. A., Cooper, C., Lane, A. W. & Riggs, B. L. (1992). *J. Bone Miner. Res*. **7**, 1005–1010.
 Miller, S. C., Bowman, B. M. & Jee, W. S. (1995). *Bone*, **17**, S117–S123.
 Nyska, M., Nyska, A., Swissa-Sivan, A. & Samueloff, S. (1995). *Int. J. Exp. Pathol*. **76**, 241–245.
 Omi, N. (2014). *J. Phys. Fitness Sports Med*. **3**, 241–248.
 Omi, N., Morikawa, N. & Ezawa, I. (2010). *J. Home Econom. Jpn*, **47**, 1173–1180.
 Prot, M., Saletti, D., Pattofatto, S., Bousson, V. & Laporte, S. (2015). *J. Biomech*. **48**, 498–503.
 Sales, E., Lima, I., de Assis, J. T., Gómez, W., Pereira, W. C. & Lopes, R. T. (2012). *Appl. Radiat. Isot*. **70**, 1272–1276.
 Snyder, A., Zierath, J. R., Hawley, J. A., Sleeper, M. D. & Craig, B. W. (1992). *Mech. Ageing Dev*. **66**, 59–69.
 Swissa-Sivan, A., Azoury, R., Statter, M., Leichter, I., Nyska, A., Nyska, M., Menczel, J. & Samueloff, S. (1990). *Calcif. Tissue Int*. **47**, 173–177.
 Swissa-Sivan, A., Simkin, A., Leichter, I., Nyska, A., Nyska, M., Statter, M., Bivas, A., Menczel, J. & Samueloff, S. (1989). *Bone Miner*. **7**, 91–105.
 Wallace, B. A. & Cumming, R. G. (2000). *Calcif. Tissue Int*. **67**, 10–18.
 Wolff, I., van Croonenborg, J. J., Kemper, H. C. G., Kostense, P. J. & Twisk, J. W. R. (1999). *Osteoporos. Int*. **9**, 1–12.
 Zhang, M. & Fan, Y. (2015). Editors. *Computational Biomechanics of the Musculoskeletal System*. Boca Raton: CRC Press.
 Zhong, W. Q. (2007). *J. Clin. Rehabil. Tissue Eng. Res*. **17**, 3351–3353.